CrossMark

Regional Amyloid-β Load and White Matter Abnormalities Contribute to Hypometabolism in Alzheimer's Dementia

Lucas Porcello Schilling [1,2,3] · Tharick A. Pascoal [1,2] · Eduardo R. Zimmer [1,2,3,4,5,6] · Sulantha Mathotaarachchi [1] · Monica Shin [1] · Carlos Roberto de Mello Rieder [3] · Serge Gauthier [1,2] · André Palmini [3] · Pedro Rosa-Neto [1,2] · for the Alzheimer's Disease Neuroimaging Initiative

Abstract

We investigated the association between amyloid-β deposition and white matter (WM) integrity as a determinant of brain glucose hypometabolism across the Alzheimer's disease (AD) spectrum. We assessed ninety-six subjects (27 cognitively normal, 49 mild cognitive impairment, and 20 AD dementia) who underwent [18F]FDG and [18F]Florbetapir positron emission tomography (PET) as well as magnetic resonance imaging (MRI) with diffusion tensor imaging. Among the regions with reduced fractional anisotropy (FA) in the AD group, we selected a voxel of interest in the angular bundle bilaterally for subsequent analyses. Using voxel-based interaction models at voxel level, we tested whether the regional hypometabolism is associated with FA in the angular bundle and regional amyloid-β deposition. In the AD patients, [18F]FDG hypometabolism in the striatum, mesiobasal temporal, orbitofrontal, precuneus, and cingulate cortices were associated with the interaction between high levels of [18F]Florbetapir standard uptake value ratios (SUVR) in these regions and low FA in the angular bundle. We found that the interaction between, rather than the independent effects of, high levels of amyloid-β deposition and WM integrity disruption determined limbic hypometabolism in patients with AD. This finding highlights a more integrative model for AD, where the interaction between partially independent processes determines the glucose hypometabolism.

Electronic supplementary material The online version of this article (https://doi.org/10.1007/s12035-018-1405-1) contains supplementary material, which is available to authorized users.

✉ Pedro Rosa-Neto
pedro.rosa@mcgill.ca

[1] Translational Neuroimaging Laboratory (TNL), McGill Center for Studies in Aging (MCSA), Douglas Mental Health Research Institute, 6825, boul. LaSalle Blvd., Montréal, QC H4H1R3, Canada

[2] Alzheimer's Disease Research Unit, MCSA, Douglas Mental Health Research Institute, Montréal, Canada

[3] Brain Institute of Rio Grande do Sul (BraIns), Pontifical Catholic University of Rio Grande do Sul (PUCRS), Porto Alegre, Brazil

[4] Department of Pharmacology, Universidade Federal do Rio Grande do Sul (UFRGS), Porto Alegre, Brazil

[5] Graduate Program in Biological Science: Biochemistry, UFRGS, Porto Alegre, Brazil

[6] Graduate Program in Biological Sciences: Pharmacology and Therapeutics, UFRGS, Porto Alegre, Brazil

Introduction

Alzheimer's disease (AD) is the most common neurodegenerative disease and the leading cause of dementia worldwide [1]. AD pathophysiology has been conceptualized as a cascade of sequential events triggered by amyloid-β deposition, followed by downstream events such as tau hyperphosphorylation, glucose hypometabolism, and eventually dementia [2–4]. However, the lack of a strong association between amyloid-β deposition and cognitive and synaptic dysfunctions has questioned whether amyloid-β deposition is a sufficient condition to trigger AD progression [5]. Indeed, recent studies have suggested that the synergistic interaction between, rather than the sequential effects of, pathological pathways such as amyloid-β and tau is the key element associated with the pathophysiological progression of AD [6].

Since the original description, AD has been characterized as a gray matter disease [7], and the most prominent pathophysiological theories of AD postulate that cortical

amyloidosis and tau accumulation underlie most neurobiological processes [8, 9]. However, the disconnection of fiber bundles has also been reported from the early stages of the disease [10, 11], suggesting that white matter (WM) abnormalities are also important in AD pathophysiology [12–15].

Diffusion tensor imaging (DTI) is a magnetic resonance imaging (MRI) technique that assesses WM organization and microstructure through fractional anisotropy (FA) [16]. In AD, WM tracts in the limbic system have shown reduced FA, suggesting loss of axons and myelin, and hence impairment in connectivity [17–20]. The pathological processes underlying such changes are still undetermined, although both Wallerian degeneration secondary to cortical neuronal loss and retrogenesis with primary axonal damage and myelin breakdown may contribute [21, 22].

[18F]Fluorodeoxyglucose ([18F]FDG) and [18F]Florbetapir positron emission tomography (PET) measure cerebral glucose metabolism and amyloid-β deposition, respectively [23, 24]. Studies in non-human primates have shed light on the relationship between WM disconnectivity and cerebral glucose metabolism in AD, showing that neurotoxic lesions in the perirhinal and entorhinal cortices lead to neocortical and hippocampal hypometabolism [25]. Subsequent human studies have correlated abnormalities in topographically related tracts to hypometabolic regions (for example, fornix FA abnormalities, and posterior cingulate cortex hypometabolism), suggesting that the progression of cerebral hypometabolism temporally follows amyloid-β deposition [26].

Such background information leaves it open whether and how these two, at least, partially independent pathophysiological processes—WM abnormalities and β-amyloid deposition—interact to determine AD progression. Here, in a cross-sectional study, we tested the hypothesis that [18F]FDG uptake reduction in limbic regions depends upon the interaction between amyloid-β deposition ([18F]Florbetapir PET SUVR) and WM integrity (FA), rather than their separated effects.

Methods

Database Description

Data used in the preparation of this article were obtained from the Alzheimer's disease Neuroimaging Initiative (ADNI) database, phases ADNIGO and ADNI2 (adni.loni.usc.edu). ADNI was launched in 2003 as a public-private partnership, led by Principal Investigator Michael W. Weiner, MD. The primary goal of ADNI has been to test whether serial MRI, PET, cerebrospinal fluid (CSF), and clinical assessment can be combined to measure the progression of mild cognitive impairment (MCI) and early AD.

Study Participants

For the present study, we only included ADNI participants who had [18F]Florbetapir, [18F]FDG, and DTI acquisitions at same visit. Cognitively normal (CN) individuals had a mini-mental state examination (MMSE) score of 24 or higher and a clinical dementia rating (CDR) of 0. MCIs had a MMSE score equal to or greater than 24, a CDR of 0.5, subjective and objective memory deficits, and essentially normal activities of daily living. AD patients had a MMSE score lower or equal 26, CDR higher than 0.5, and met the National Institute of Neurological and Communicative Disorders and Stroke-Alzheimer's Disease and Related Disorders Association criteria for probable AD [27]. All individuals had absence of any other neuropsychiatric disorders. Importantly, the ADNI study was approved by the Institutional Review Boards (IRBs) of each participating site and was conducted in accordance with Federal Regulations, the Internal Conference on Harmonization (ICH), and good clinical practices (GCP). The ADNI Research Committee has approved all the protocols used in the study. The study subjects provided written informed consent at the time of enrollment for imaging and completed questionnaires that were approved by each participating site's IRB. Further information regarding the ADNI inclusion/exclusion criteria are described in detail at www.adni-info.org [accessed November 2016].

DTI Methods

The images were acquired conforming ADNI protocols (www.adni-info.org[accessed November 2016]). Briefly, all diffusion images were scanned on 3 Tesla (3 T) GE Medical Systems scanners. Scans comprised of 41 diffusion encoding and five resting (b0) directions. A voxel size of 1.4 mm × 1.4 mm × 2.7 mm and $b = 1000$ s/mm^2 was used. All scans used in this study were corrected for EPI current. T1 scans were acquired on the same GE 3 T scanner with a 1.2 mm × 1 mm × 1 mm voxel size. Further acquisition details are available from ADNI website (ADNI-INFO.org). After processing the DTIs, FA maps were generated using FSL-DTIFIT from the skull-stripped eddy current corrected images in the native MRI space (Fig. 1). A statistical comparison of voxel-wise FA values was performed to identify the differences between each diagnostic group (Fig. 2). The anatomical WM bundles have been identified by the MRI Atlas of human white matter. For the subsequent analysis, the angular bundle was defined a prior, since it is a well-defined tract related to AD dementia, which directly connects the hippocampus to the entorhinal cortex. A voxel-of-interest (VOI) was obtained from the angular bundle bilaterally and was used to extract FA values from each subject (see supplementary information).
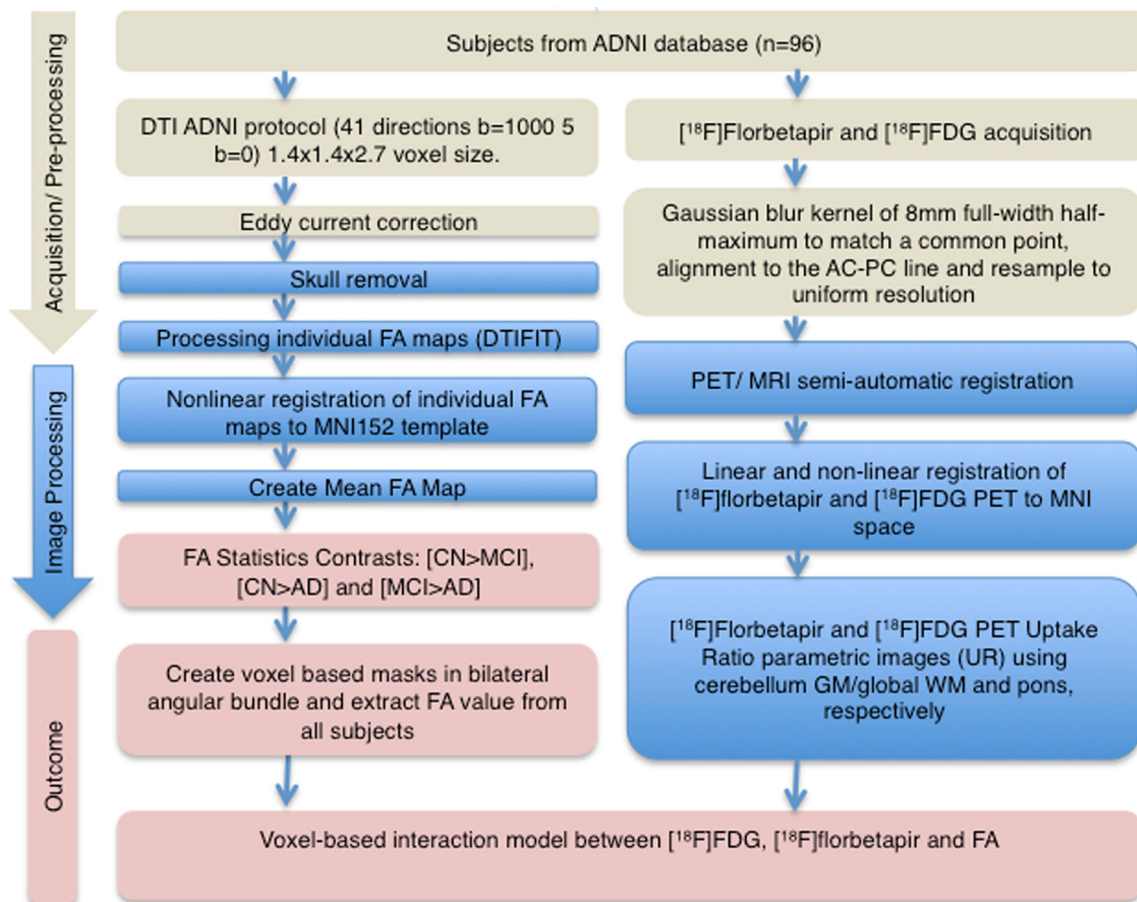
Fig. 1 Summary of image analysis methods

PET Methods

PET images were acquired following the ADNI acquisition protocols (http://adni.loni.usc.edu/methods, accessed in January 2016). Imaging analysis methods are summarized in Fig. 1. In summary, during the pre-processing stage, the acquired images were blurred to match a common point spread function of 8-mm full-width half–maximum Gaussian kernel, aligned to the AC-PC line, and resampled to achieve a common uniform resolution. Subsequently, in the post-processing stage, the images underwent non-linear spatial normalization to the MNI 152 template space using the transformation derived from the automatic PET/T1-MRI transformation and anatomical MRI registration for each subject. Voxel-wise standardized uptake value ratio (SUVR) images were generated for [^{18}F]Florbetapir and [^{18}F]FDG using the cerebellum gray matter/global white matter and pons as the reference regions, respectively. A global PET SUVR value for each subject was estimated using a composite of the precuneus, prefrontal, orbitofrontal, parietal, temporal, anterior, and posterior cingulate cortices.

Statistical Methods

The analyses were performed using Matlab® (http://www.mathworks.com; accessed November 2016) with a novel computational platform developed to perform complex voxel–wise statistical operations, such as interaction models, with different imaging modalities [28].

First, we compared the FA between CN and AD groups and identified clusters of FA reduction in the bilateral angular bundle and the fornix (Fig. 2). After correcting for multiple comparisons (false discovery rate at $p < 0.05$), we extracted the FA values in VOIs in bilateral angular bundles for the subsequent analyses.

To evaluate whether the interaction between WM abnormalities (FA in bilateral angular bundle) and amyloid-β deposition ([^{18}F]Florbetapir SUVR at every voxel) determines the regional hypometabolism, we used the following statistical model:

$$FDG = \beta 0 + \beta 1(\text{Florbetapir}) + \beta 2(\text{FA})$$
$$+ \beta 3(\text{Florbetapir*FA}) + \text{covariates} + \text{error}$$

Fig. 2 Regional diagnostic effect on fractional anisotropy. Statistical parametrical maps represent areas of reduced FA in patients with AD ($n = 20$) as compared to CN ($n = 27$). FA reduction was found in parahippocampal WM, angular bundle, and fornix regions (data false discovery rate corrected at $P < 0.05$). AD, Alzheimer's disease; CN, cognitively normal; FA, fractional anisotropy; WM, white matter

Results
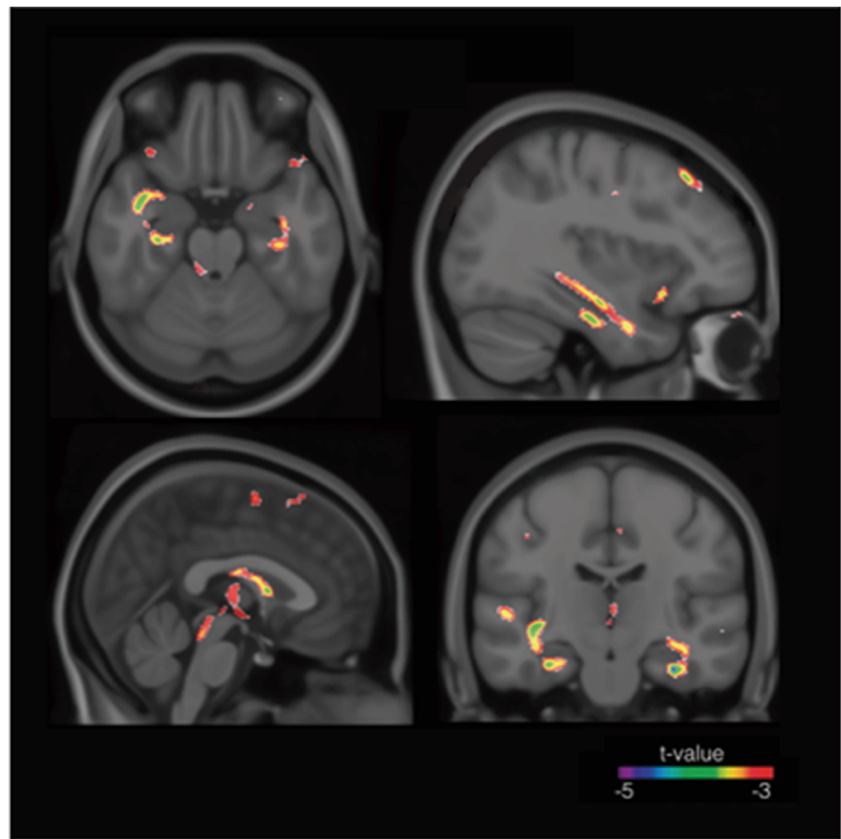
The model was adjusted for Hachinski score [29] to limit the impact of vascular WM load, age, gender, education, and APOE ε4 status. The statistical parametric maps were corrected for multiple comparisons using false discovery rate at $p < 0.05$ [30].

Results

Demographic features are summarized in Table 1. The CN group has [18F]Florbetapir global mean SUVR of 1.10 (standard deviation [SD] = 0.14), [18F]FDG global mean SUVR 1.20 ([SD] = 0.11). The CN group has [18F]Florbetapir global mean SUVR of 1.19 [SD = 0.15], [18F]FDG global mean 1.20 [SD = 0.10]. The AD group has [18F]Florbetapir global mean SUVR mean of 1.37 [SD = 0.23] and [18F]FDG global mean SUVR of 1.156 [SD = 0.14]. The [18F]FDG and [18F]Florbetapir group statistical comparisons are summarized in Table 2.

Patients with AD had significantly reduced FAs in the angular bundle bilaterally and in the fornix compared to CN ($P < 0.05$) (Fig. 2), but not in relation to the MCI group. Since WM abnormalities on the angular bundle were related to a diagnosis of AD dementia, a VOI was defined in this region for the subsequent analysis. Importantly, the three diagnostic groups showed distinct averaged FA values in the VOI bilaterally. The CN group had the highest values, with statistical significance between CN and AD (left angular bundle (LAB) mean = 0.14 [SD = 0.03]; CN–AD: $P = 0.10$; CN–MCI: $P = 0.45$; and right angular bundle (RAB) mean = 0.16 [SD = 0.02]; CN–AD: $P = 0.01$; CN–MCI: $P = 0.11$). The AD group had non-statistical significant lower FAs (LAB mean = 0.12 [SD = 0.02], RAB mean = 0.12 [SD = 0.02]) compared to MCI group (LAB mean = 0.13 [SD = 0.04], $P = 0.46$; RAB mean = 0.14 [SD = 0.04], $P = 0.19$).

In the AD group, a voxel-based analysis revealed that [18F]FDG hypometabolism in the striatum, basal and mesial temporal, orbitofrontal, precuneus, anterior, and posterior cingulate cortices were driven by the interaction between high levels of [18F]Florbetapir uptake in these regions and low FA in the angular bundle (Fig. 3). Moreover, the laterality of the angular bundle VOI was associated with distinct patterns of regional hypometabolism. The interaction of RAB disconnections with amyloid-β deposition was associated with [18F]FDG hypometabolism in the precuneus and posterior cingulate cortex (Fig. 3a), while disconnections in the LAB were associated with the striatum, basal and mesial temporal, orbitofrontal, and anterior cingulate cortices [18F]FDG hypometabolism (Fig. 3b). Notably, this interaction was not found in the CN and MCI groups.

Table 1 Demographics and key characteristics of the population

Characteristics	All	Control	MCI	AD
No.	96	27	49	20
Age, year, mean (SD)	73.81 (6.51)	74.4 (6.2)	73.1 (6.5)	74.5 (6.9)
Male, no. (%)	62 (64)	16 (59)	33 (67)	13 (65)
APOE ε4 carriers, no. (%)	55 (57)	11 (40)	30 (61)	14 (70)
Education, year, mean (SD)	16.39 (2.74)	16.9 (2.8)	16.1 (2.5)	16.2 (2.9)
MMSE, score, mean (SD)	27.14 (2.68)	28.6 (1.5)	27.9 (1.6)	23.2 (2.1)
Hachinski score (SD)	0.71 (0.70)	0.70 (0.46)	0.73 (0.72)	0.7 (0.92)
CDR score, mean (SD)	0.42 (0.31)	0 (0)	0.5 (0)	0.8 (0.25)
[18F]FDG, mean SUVR (SD)	1.18 (0.12)	1.20 (0.11)	1.20 (0.10)	1.11 (0.14)
[18F]Florbetapir, mean SUVR (SD)	1.20 (0.19)	1.10 (0.14)	1.19 (0.15)	1.37 (0.23)

AD, Alzheimer disease; *CDR*, clinical dementia rating; *[18F]FDG*, [18F]fluorodeoxyglucose; *MCI*, mild cognitive impairment; *MMSE*, mini-mental state examination; *SD*, standard deviation; *SUVR*, standardized uptake value ratio

Discussion

We showed that the interaction between amyloid-β accumulation and FA reduction in the angular bundle is significantly associated with hypometabolism in limbic regions in patients with AD dementia.

Overall, this finding is in agreement with an integrative framework proposing that the co-occurrence of different pathophysiological processes potentiates neurodegeneration and clinical progression in AD [6, 31–33]. As previously shown, we found decreased FA values in WM tracts associated with the memory system, including the angular bundle and the fornix [34–36]. Microstructural WM damage disrupts connections to cortical areas, as observed in regional changes in the parahippocampal WM, leading to mesial temporal lobe deafferentation [37]. Most abnormalities are found in temporal lobe regions, with frequent targets in the retrogenesis model of WM impairment in AD. Previous reports have shown associations between reduced FA and both regional glucose hypometabolism, particularly of the posterior cingulate cortex, and the volume of the descending cingulum [38, 39]. The hippocampal atrophy, also a neurodegenerative

radiological feature of AD, has been also related with decreased FA [40]. The posterior cingulate cortex metabolism was also inversely related to diffusivity increase in the hippocampus [41]. Assessing the temporal relationship between biomarkers, Villain and colleagues posit that hippocampal atrophy leads to the disruption of the cingulum bundle and cingulate fasciculus, with subsequent glucose hypometabolism in these areas [42, 43].

Whereas biomarkers of neurodegeneration and WM disruption have been previously correlated, similar findings have not been observed in regard to amyloid-β deposition PET imaging in pre-dementia subjects [40]. In our interaction study, we found hypometabolic areas related to angular bundle abnormalities and also to amyloid-β deposition in the AD group. Interestingly, these regions are described in Braak's neuropathological stages B and C involving isocortex association areas, in patients with significant clinical decline [9]. These findings suggest a possible increase metabolic vulnerability to the interaction of the posterior limbic structures in the right non-dominant hemisphere, and in the anterior and basal nuclei areas in the dominant left hemisphere.

The relationship between CSF biomarkers (Aβ$_{1-42}$ and p-Tau181) and WM integrity has been studied in CN adults, and a positive correlation was found between the Aβ$_{1-42}$/p-Tau181 ratio and FA in the fornix, corpus callosum, and inferior, superior, and inferior fronto-occipital fasciculus [44]. Furthermore, significantly, reduced FA in the left posterior cingulum was observed in patients with pathological CSF total tau levels [45], and the concentration of Aβ$_{1-42}$ has been directly correlated with mean FA values [46]. In fact, decreased FA has been reported in frontotemporal dementia and dementia with Lewy bodies [47, 48]. Interestingly, amyloid PET positive asymptomatic subjects have been shown to display increased FA, suggesting a compensatory mechanism in very early stages of the disease by glial response and axonal pruning at regions of crossing fibers [49]. We speculate that

Table 2 PET FDG and Florbetapir SUVR global comparisons

PET Global SUVR Comparisons	*P* value
[18F]Florbetapir: CN—MCI	0.2
[18F]Florbetapir: CN—AD	0.01
[18F]Florbetapir: MCI—AD	0.01
[18F]FDG: CN—MCI	0.97
[18F]FDG: CN—AD	0.08
[18F]FDG: MCI—AD	0.02

AD, Alzheimer disease; *[18F]FDG*, [18F]fluorodeoxyglucose; *MCI*, mild cognitive impairment; *SD*, standard deviation; *SUVR*, standardized uptake value ratio
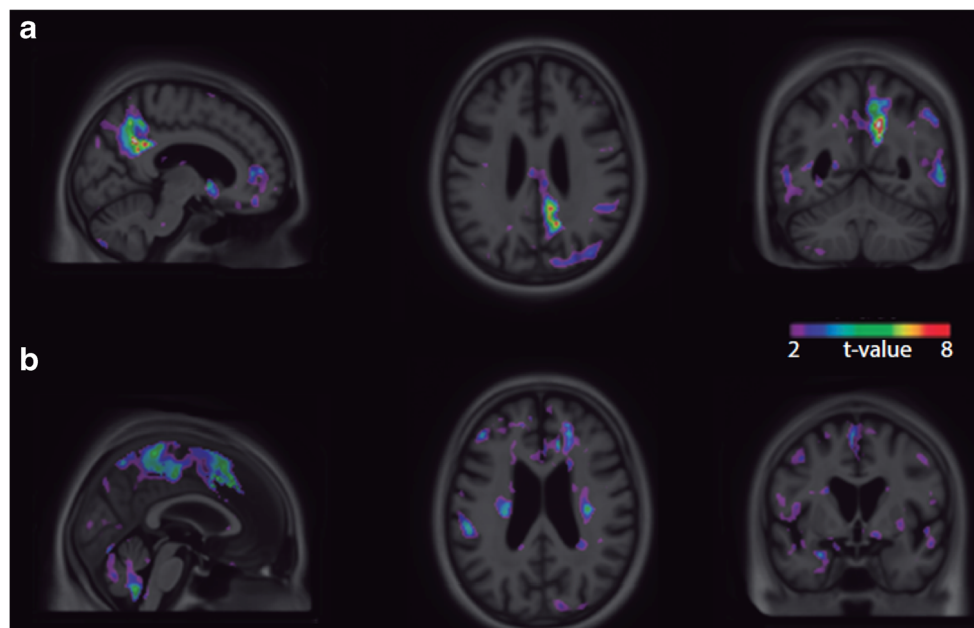
Fig. 3 The interaction between amyloid-β deposition and WM integrity disruption determines limbic hypometabolism in patients with AD. (**a**) Statistical parametric maps (false discovery rate corrected at $P < 0.05$) overlaid on a structural MRI scan reveal areas where [18F]FDG uptake declined as a function of the interaction between [18F]Florbetapir SUVR at every voxel and FA in the right angular bundle. Significant interactive effects between [18F]Florbetapir SUVR and FA were observed in the right precuneus and posterior cingulate cortex in the AD group ($n = 20$). (**b**) Statistical parametric maps (false discovery rate corrected at $P < 0.05$) overlaid on a structural MRI scan, reveal areas where [18F]FDG uptake declined as a function of the interaction between [18F]Florbetapir SUVR at every voxel and FA in the left angular bundle. Significant interactive effects between [18F]Florbetapir SUVR and FA were observed in the left striatum, mesial temporal, orbitofrontal, and anterior cingulate cortices in the AD group ($n = 20$). AD, Alzheimer's disease; FA, fractional anisotropy; [18F]FDG, [18F]Fluorodeoxyglucose; MRI, magnetic resonance imaging; SUVR, standardized uptake value ratio

the latter mechanism may explain the non-significant results observed in our CN and "pre-dementia" MCI patients. Further studies with a larger number of asymptomatic and MCI subjects, with enriched amyloid tau status subjects, may help to elucidate these questions and capture group differences.

Importantly, previous studies did not observe strong associations between regional amyloid-β deposition and glucose hypometabolism in AD patients [50]. Here, we have shown that the interaction with white matter integrity disruption is the key element linking regional glucose hypometabolism and amyloid pathology in the dementia phase of AD.

Integrating distinct modalities may foster a better understanding of the mechanisms underlying AD progression, beyond the role of individual biomarkers. It has been shown that amyloid status combined with CSF tau levels, and also with baseline cerebral metabolic decline, predicts conversion to dementia in patients with MCI [51–53]. Therefore, integrative biomarker studies may offer a new avenue to evaluate individual risks of progression along the cognitive continuum of aging. Specifically, since the interaction with WM disruption is the key element linking amyloid-β and pathophysiological progression in AD, we may argue that our results suggest that the use of biomarkers of WM integrity could help to identify those fated to develop dementia symptoms among MCIs with amyloid-β pathology.

The major methodological strength of our study is the use of only continuous biomarker values. Biomarkers occur on a continuum; therefore, dichotomization techniques are invariably subject to analytical and methodological idiosyncrasies. Some methodological issues limit the interpretation of our results. The cross-sectional analysis prevents inferences on the progression of WM abnormalities, amyloid deposition, and glucose metabolism. It is also important to highlight that FDG SUVR measurement is sensitive to several biological factors such as blood glucose levels, physical, and synaptic activity.

Also, because patients had to have performed the complete imaging protocol, we included a relatively small number of AD subjects, and thus our main findings need confirmation in larger samples. Despite the limited number of subjects, in order to avoid potential confounding effects, we performed all the statistical analyses including covariates that could impact the results, as age, gender, vascular WM load, education, and APOE $\varepsilon 4$ status. Notwithstanding these limitations, our results show that combining glucose metabolism, amyloid-β, and WM integrity in relevant brain regions offers the encouraging possibility to assess different pathological processes in the same patient at the same time. More importantly, the integration of different biomarkers in sophisticated statistical models may help clarify the pathological alterations observed along the AD spectrum.

Conclusion

In sum, the major result of our study demonstrates a strong association between amyloid-β deposition and glucose hypometabolism through a synergistic interaction with white matter disruption. These results support a more integrative model for AD progression, suggesting that the convergence of partially independent pathological pathways drives disease progression. These findings provide novel insights in AD pathophysiology framework by suggesting that future disease–modifying therapies using [^{18}F]FDG as a biomarker for efficacy should integrate measures of white matter integrity in order to better interpret the therapeutic effects of the intervention.

USA. [58]Ohio State University, Ohio, USA. [59]Albany Medical College, NY, USA. [60]Hartford Hospital, Olin Neuropsychiatry Research Center, Connecticut, USA. [61]Dartmouth-Hitchcock Medical Center, New Hampshire, USA. [62]Wake Forest University Health Sciences, North Carolina, USA. [63]Rhode Island Hospital, state of Rhode Island, USA. [64]Butler Hospital, Providence, Rhode Island, USA. [65]University of California, San Francisco, USA. [66]Medical University South Carolina, USA. [67]Nathan Kline Institute, Orangeburg, New York, USA. [68]Cornell University, Ithaca, New York, USA. [69]USF Health Byrd Alzheimer's Institute, University of South Florida, USA.

Compliance with Ethical Standards

Conflict of interest The authors declare that they have no conflict of interest.

Abbreviations AD, Alzheimer's disease; ADNI, Alzheimer's disease neuroimaging initiative; CDR, clinical dementia rating; CN, cognitive normal; FA, fractional anisotropy; LAB, left angular bundle; [18F]FDG, [18F]fluorodeoxyglucose; MCI, mild cognitive impairment; MMSE, mini-mental state examination; MRI, magnetic resonance imaging; RAB, right angular bundle; SD, standard deviation; SUVR, standardized uptake value ratio; VOI, voxel of interest; WM white matter

References

1. Alzheimer's A (2016) 2016 Alzheimer's disease facts and figures. Alzheimers Dement 12(4):459–509
2. Hardy J, Selkoe DJ (2002) The amyloid hypothesis of Alzheimer's disease: progress and problems on the road to therapeutics. Science 297(5580):353–356. https://doi.org/10.1126/science.1072994
3. Jack CR Jr, Knopman DS, Jagust WJ, Petersen RC, Weiner MW, Aisen PS, Shaw LM, Vemuri P et al (2013) Tracking pathophysiological processes in Alzheimer's disease: an updated hypothetical model of dynamic biomarkers. Lancet Neurol 12(2):207–216. https://doi.org/10.1016/S1474-4422(12)70291-0
4. Sperling RA, Aisen PS, Beckett LA, Bennett DA, Craft S, Fagan AM, Iwatsubo T, Jack CR Jr et al (2011) Toward defining the preclinical stages of Alzheimer's disease: recommendations from the National Institute on Aging-Alzheimer's Association workgroups on diagnostic guidelines for Alzheimer's disease. Alzheimers Dement 7(3):280–292. https://doi.org/10.1016/j.jalz.2011.03.003
5. Altmann A, Ng B, Landau SM, Jagust WJ, Greicius MD, Alzheimer's Disease Neuroimaging I (2015) Regional brain hypometabolism is unrelated to regional amyloid plaque burden. Brain 138(Pt 12):3734–3746. https://doi.org/10.1093/brain/awv278
6. Pascoal TA, Mathotaarachchi S, Mohades S, Benedet AL, Chung CO, Shin M, Wang S, Beaudry T et al (2016) Amyloid-beta and hyperphosphorylated tau synergy drives metabolic decline in preclinical Alzheimer's disease. Mol Psychiatry 22:306–311. https://doi.org/10.1038/mp.2016.37
7. Cipriani G, Dolciotti C, Picchi L, Bonuccelli U (2011) Alzheimer and his disease: a brief history. Neurol Sci 32(2):275–279. https://doi.org/10.1007/s10072-010-0454-7
8. Hardy JA, Higgins GA (1992) Alzheimer's disease: the amyloid cascade hypothesis. Science 256(5054):184–185
9. Braak H, Braak E (1991) Neuropathological stageing of Alzheimer-related changes. Acta Neuropathol 82(4):239–259
10. Rose SE, Chen F, Chalk JB, Zelaya FO, Strugnell WE, Benson M, Semple J, Doddrell DM (2000) Loss of connectivity in Alzheimer's disease: an evaluation of white matter tract integrity with colour coded MR diffusion tensor imaging. J Neurol Neurosurg Psychiatry 69(4):528–530
11. Bozzali M, Falini A, Franceschi M, Cercignani M, Zuffi M, Scotti G, Comi G, Filippi M (2002) White matter damage in Alzheimer's disease assessed in vivo using diffusion tensor magnetic resonance imaging. J Neurol Neurosurg Psychiatry 72(6):742–746
12. de la Monte SM (1989) Quantitation of cerebral atrophy in preclinical and end-stage Alzheimer's disease. Ann Neurol 25(5):450–459. https://doi.org/10.1002/ana.410250506
13. Medina D, DeToledo-Morrell L, Urresta F, Gabrieli JD, Moseley M, Fleischman D, Bennett DA, Leurgans S et al (2006) White matter changes in mild cognitive impairment and AD: a diffusion tensor imaging study. Neurobiol Aging 27(5):663–672. https://doi.org/10.1016/j.neurobiolaging.2005.03.026
14. Zhang Y, Schuff N, Jahng GH, Bayne W, Mori S, Schad L, Mueller S, Du AT et al (2007) Diffusion tensor imaging of cingulum fibers in mild cognitive impairment and Alzheimer disease. Neurology 68(1):13–19. https://doi.org/10.1212/01.wnl.0000250326.77323.01
15. Nowrangi MA, Lyketsos CG, Leoutsakos JM, Oishi K, Albert M, Mori S, Mielke MM (2013) Longitudinal, region-specific course of diffusion tensor imaging measures in mild cognitive impairment and Alzheimer's disease. Alzheimer's Dement 9(5):519–528. https://doi.org/10.1016/j.jalz.2012.05.2186
16. Pierpaoli C, Basser PJ (1996) Toward a quantitative assessment of diffusion anisotropy. Magn Reson Med 36(6):893–906
17. Le Bihan D, Mangin JF, Poupon C, Clark CA, Pappata S, Molko N, Chabriat H (2001) Diffusion tensor imaging: concepts and applications. J Magn Reson Imaging 13(4):534–546
18. Chua TC, Wen W, Slavin MJ, Sachdev PS (2008) Diffusion tensor imaging in mild cognitive impairment and Alzheimer's disease: a review. Curr Opin Neurol 21(1):83–92. https://doi.org/10.1097/WCO.0b013e3282f4594b
19. Bartzokis G, Cummings JL, Sultzer D, Henderson VW, Nuechterlein KH, Mintz J (2003) White matter structural integrity in healthy aging adults and patients with Alzheimer disease: a magnetic resonance imaging study. Arch Neurol 60(3):393–398
20. Fellgiebel A, Muller MJ, Wille P, Dellani PR, Scheurich A, Schmidt LG, Stoeter P (2005) Color-coded diffusion-tensor-imaging of posterior cingulate fiber tracts in mild cognitive impairment. Neurobiol Aging 26(8):1193–1198. https://doi.org/10.1016/j.neurobiolaging.2004.11.006
21. Reisberg B, Franssen EH, Hasan SM, Monteiro I, Boksay I, Souren LE, Kenowsky S, Auer SR et al (1999) Retrogenesis: clinical, physiologic, and pathologic mechanisms in brain aging, Alzheimer's and other dementing processes. Eur Arch Psychiatry Clin Neurosci 249(Suppl 3):28–36
22. Brun A, Gustafson L, Englund E (1990) Subcortical pathology of Alzheimer's disease. Adv Neurol 51:73–77
23. Schilling LP, Leuzy A, Zimmer ER, Gauthier S, Rosa-Neto P (2014) Nonamyloid PET biomarkers and Alzheimer's disease: current and future perspectives. Future Neurol 9(6):597–613
24. Schilling LP, Zimmer ER, Shin M, Leuzy A, Pascoal TA, Benedet AL, Borelli WV, Palmini A et al (2016) Imaging Alzheimer's disease pathophysiology with PET. Dement Neuropsychol 10(2):79–90
25. Meguro K, Blaizot X, Kondoh Y, Le Mestric C, Baron JC, Chavoix C (1999) Neocortical and hippocampal glucose hypometabolism following neurotoxic lesions of the entorhinal and perirhinal cortices in the non-human primate as shown by PET. Implications for Alzheimer's disease. Brain 122(Pt 8):1519–1531

26. Forster S, Grimmer T, Miederer I, Henriksen G, Yousefi BH, Graner P, Wester HJ, Forstl H et al (2012) Regional expansion of hypometabolism in Alzheimer's disease follows amyloid deposition with temporal delay. Biol Psychiatry 71(9):792–797. https://doi.org/10.1016/j.biopsych.2011.04.023

27. McKhann G, Drachman D, Folstein M, Katzman R, Price D, Stadlan EM (1984) Clinical diagnosis of Alzheimer's disease: report of the NINCDS-ADRDA work group under the auspices of Department of Health and Human Services Task Force on Alzheimer's disease. Neurology 34(7):939–944

28. Mathotaarachchi S, Wang S, Shin M, Pascoal TA, Benedet AL, Kang MS, Beaudry T, Fonov VS et al (2016) VoxelStats: a MATLAB package for multi-modal voxel-wise brain image analysis. Front Neuroinform 10:20. https://doi.org/10.3389/fninf.2016.00020

29. Hachinski VC, Iliff LD, Zilhka E, Du Boulay GH, McAllister VL, Marshall J, Russell RW, Symon L (1975) Cerebral blood flow in dementia. Arch Neurol 32(9):632–637

30. Benjamini; Y, Hochberg Y (1995) Controlling the false discovery rate: a practical and powerful approach to multiple testing. J R Stat Soc Ser B 57(1):289–300

31. Duyckaerts C (2011) Tau pathology in children and young adults: can you still be unconditionally baptist? Acta Neuropathol 121(2):145–147. https://doi.org/10.1007/s00401-010-0794-7

32. Mesulam MM (1999) Neuroplasticity failure in Alzheimer's disease: bridging the gap between plaques and tangles. Neuron 24(3):521–529

33. Small SA, Duff K (2008) Linking Abeta and tau in late-onset Alzheimer's disease: a dual pathway hypothesis. Neuron 60(4):534–542. https://doi.org/10.1016/j.neuron.2008.11.007

34. Mielke MM, Kozauer NA, Chan KC, George M, Toroney J, Zerrate M, Bandeen-Roche K, Wang MC et al (2009) Regionally-specific diffusion tensor imaging in mild cognitive impairment and Alzheimer's disease. NeuroImage 46(1):47–55. https://doi.org/10.1016/j.neuroimage.2009.01.054

35. Agosta F, Pievani M, Sala S, Geroldi C, Galluzzi S, Frisoni GB, Filippi M (2011) White matter damage in Alzheimer disease and its relationship to gray matter atrophy. Radiology 258(3):853–863. https://doi.org/10.1148/radiol.10101284

36. Rowley J, Fonov V, Wu O, Eskildsen SF, Schoemaker D, Wu L, Mohades S, Shin M et al (2013) White matter abnormalities and structural hippocampal disconnections in amnestic mild cognitive impairment and Alzheimer's disease. PLoS One 8(9):e74776. https://doi.org/10.1371/journal.pone.0074776

37. Salat DH, Tuch DS, van der Kouwe AJ, Greve DN, Pappu V, Lee SY, Hevelone ND, Zaleta AK et al (2010) White matter pathology isolates the hippocampal formation in Alzheimer's disease. Neurobiol Aging 31(2):244–256. https://doi.org/10.1016/j.neurobiolaging.2008.03.013

38. Kochunov P, Ramage AE, Lancaster JL, Robin DA, Narayana S, Coyle T, Royall DR, Fox P (2009) Loss of cerebral white matter structural integrity tracks the gray matter metabolic decline in normal aging. NeuroImage 45(1):17–28. https://doi.org/10.1016/j.neuroimage.2008.11.010

39. Bozoki AC, Korolev IO, Davis NC, Hoisington LA, Berger KL (2012) Disruption of limbic white matter pathways in mild cognitive impairment and Alzheimer's disease: a DTI/FDG-PET study. Hum Brain Mapp 33(8):1792–1802. https://doi.org/10.1002/hbm.21320

40. Kantarci K, Schwarz CG, Reid RI, Przybelski SA, Lesnick TG, Zuk SM, Senjem ML, Gunter JL et al (2014) White matter integrity determined with diffusion tensor imaging in older adults without dementia: influence of amyloid load and neurodegeneration. JAMA Neurol 71(12):1547–1554. https://doi.org/10.1001/jamaneurol.2014.1482

41. Yakushev I, Schreckenberger M, Muller MJ, Schermuly I, Cumming P, Stoeter P, Gerhard A, Fellgiebel A (2011) Functional implications of hippocampal degeneration in early Alzheimer's disease: a combined DTI and PET study. Eur J Nucl Med Mol Imaging 38(12):2219–2227. https://doi.org/10.1007/s00259-011-1882-1

42. Villain N, Desgranges B, Viader F, de la Sayette V, Mezenge F, Landeau B, Baron JC, Eustache F et al (2008) Relationships between hippocampal atrophy, white matter disruption, and gray matter hypometabolism in Alzheimer's disease. J Neurosci 28(24):6174–6181. https://doi.org/10.1523/JNEUROSCI.1392-08.2008

43. Villain N, Fouquet M, Baron JC, Mezenge F, Landeau B, de La Sayette V, Viader F, Eustache F et al (2010) Sequential relationships between grey matter and white matter atrophy and brain metabolic abnormalities in early Alzheimer's disease. Brain 133(11):3301–3314. https://doi.org/10.1093/brain/awq203

44. Gold BT, Zhu Z, Brown CA, Andersen AH, LaDu MJ, Tai L, Jicha GA, Kryscio RJ et al (2014) White matter integrity is associated with cerebrospinal fluid markers of Alzheimer's disease in normal adults. Neurobiol Aging 35(10):2263–2271. https://doi.org/10.1016/j.neurobiolaging.2014.04.030

45. Stenset V, Bjornerud A, Fjell AM, Walhovd KB, Hofoss D, Due-Tonnessen P, Gjerstad L, Fladby T (2011) Cingulum fiber diffusivity and CSF T-tau in patients with subjective and mild cognitive impairment. Neurobiol Aging 32(4):581–589. https://doi.org/10.1016/j.neurobiolaging.2009.04.014

46. Li X, Li TQ, Andreasen N, Wiberg MK, Westman E, Wahlund LO (2014) The association between biomarkers in cerebrospinal fluid and structural changes in the brain in patients with Alzheimer's disease. J Intern Med 275(4):418–427. https://doi.org/10.1111/joim.12164

47. Zhang Y, Schuff N, Du AT, Rosen HJ, Kramer JH, Gorno-Tempini ML, Miller BL, Weiner MW (2009) White matter damage in frontotemporal dementia and Alzheimer's disease measured by diffusion MRI. Brain 132(Pt 9):2579–2592. https://doi.org/10.1093/brain/awp071

48. Kantarci K, Avula R, Senjem ML, Samikoglu AR, Zhang B, Weigand SD, Przybelski SA, Edmonson HA et al (2010) Dementia with Lewy bodies and Alzheimer disease: neurodegenerative patterns characterized by DTI. Neurology 74(22):1814–1821. https://doi.org/10.1212/WNL.0b013e3181e0f7cf

49. Racine AM, Adluru N, Alexander AL, Christian BT, Okonkwo OC, Oh J, Cleary CA, Birdsill A et al (2014) Associations between white matter microstructure and amyloid burden in preclinical Alzheimer's disease: a multimodal imaging investigation. Neuroimage Clin 4:604–614. https://doi.org/10.1016/j.nicl.2014.02.001

50. Wirth M, Madison CM, Rabinovici GD, Oh H, Landau SM, Jagust WJ (2013) Alzheimer's disease neurodegenerative biomarkers are associated with decreased cognitive function but not beta-amyloid in cognitively normal older individuals. J Neurosci 33(13):5553–5563. https://doi.org/10.1523/JNEUROSCI.4409-12.2013

51. Hansson O, Zetterberg H, Buchhave P, Londos E, Blennow K, Minthon L (2006) Association between CSF biomarkers and incipient Alzheimer's disease in patients with mild cognitive impairment: a follow-up study. Lancet Neurol 5(3):228–234. https://doi.org/10.1016/S1474-4422(06)70355-6

52. Okello A, Koivunen J, Edison P, Archer HA, Turkheimer FE, Nagren K, Bullock R, Walker Z et al (2009) Conversion of amyloid positive and negative MCI to AD over 3 years: an 11C-PIB PET study. Neurology 73(10):754–760. https://doi.org/10.1212/WNL.0b013e3181b23564

53. Buchhave P, Minthon L, Zetterberg H, Wallin AK, Blennow K, Hansson O (2012) Cerebrospinal fluid levels of beta-amyloid 1-42, but not of tau, are fully changed already 5 to 10 years before the onset of Alzheimer dementia. Arch Gen Psychiatry 69(1):98–106. https://doi.org/10.1001/archgenpsychiatry.2011.155